

# RXTE observations of the Seyfert galaxy NGC 5506: evidence for reflection from disk and torus

G. Lamer,<sup>★</sup> P.Uttley, and I.M. M<sup>c</sup>Hardy

<sup>1</sup>Department of Physics and Astronomy, The University, Southampton, SO17 1BJ

Accepted. Received

## ABSTRACT

We report on observations of the narrow line Seyfert galaxy NGC 5506 with the *Rossi X-ray timing explorer*. The observations cover a time interval of  $\sim 1000$  days during which the source showed strong flux and spectral variability. The spectrum clearly shows iron fluorescence emission at 6.4 keV and significant reflection features. Both the equivalent width of the iron line and the relative strength of the reflected continuum are higher during low flux states. The variability of the reflection features can be explained by the presence of two reflected components: one that responds rapidly to flux changes of the primary continuum and a second, slowly variable, component originating from a distant reflector, e.g. a molecular torus.

**Key words:** Galaxies: individual: NGC 5506 – X-rays: galaxies – Galaxies: Seyferts

## 1 INTRODUCTION

NGC 5506 is a bright nearby ( $z=0.006$ ) narrow emission line X-ray galaxy. It has been classified variously as edge on early type spiral (de Vaucouleurs et al. 1976) and irregular (Wilson et al. 1976, Wilson et al. 1985). Strong nuclear dust lanes as well as starburst activity are present in this galaxy. Although the optical spectrum of the nucleus is classified as Seyfert 2, NGC 5506 is not a typical member of this subclass. All spectral components, including the narrow lines, are strongly reddened by the disk of the host galaxy. The X-ray source is absorbed by a column of  $N_{\text{H}} = 3.6 \cdot 10^{22}$  (Perola 1998). This column is moderate for a Seyfert 2 nucleus and might be largely due to absorption by interstellar matter in the edge-on galaxy, rather than absorption by a nuclear torus. Despite this relatively low absorption in X-rays, no broad line region has been unambiguously detected in near infrared observations (Veilleux et al. 1997). Goodrich et al. (1994) conclude that the relative broadening of the NIR lines relative to the optical lines is due to a contribution from the inner parts of the narrow line region that is reddened by the dust lane crossing the bulge of NGC 5506.

The 2-30 keV X-ray spectra of Seyfert galaxies are dominated by two components: a power law component that is believed to originate from the primary source of hard X-rays near the central black hole and a reflected component produced by Compton scattering of the primary radiation by neutral material (eg Pounds et al. 1990). The principal spectral signatures of the reflected component are a broad hump peaking at  $\sim 30$  keV and iron  $K_{\alpha}$  fluorescence emission at 6.4 keV. The strength of the broad hump is more or less independent of the relative abundances but the strength of the iron feature depends directly on the iron abundance.

In many Seyfert X-ray spectra a broad, gravitationally redshifted iron fluorescence line is present, indicating that the reflection at least partly occurs in the accretion disk, (Tanaka et al. 1995, Nandra et al. 1997, Reynolds & Begelman 1997). However, Ghisellini et al. (1994) and Krolik et al. (1994) showed that the molecular torus required by unified models of Seyfert galaxies is also likely to modify the X-ray spectra of both Seyfert 1 and Seyfert 2 galaxies by reprocessing the primary radiation. The molecular torus is the supposed origin of narrow iron  $K_{\alpha}$  components found in the *ASCA* spectra of several Seyfert galaxies (Weaver et al. 1997, Yaqoob et al. 1996, Weaver & Reynolds 1998). Any reflection component originating from the torus will respond only slowly to variations of the primary X-ray source and therefore its *relative* contribution to the X-ray spectrum will be anti-correlated with the flux from the variable X-ray source. Due to this temporal behaviour reprocessing by a distant reflector can be identified using long term monitoring X-ray observations. The presence of an obviously distant reflector in the Seyfert 1 galaxy NGC 4051 was revealed when a “bare” reflection component became visible while the primary X-ray source virtually switched off for  $\sim 150$  days (Guainazzi et al. 1998, Uttley et al. 1999).

In this paper we present X-ray monitoring observations of NGC 5506 obtained with the *Rossi X-ray Timing Explorer* (*RXTE*) as well as a 100 ksec *RXTE* observation spread over 20 days in June/July 1997. The reflection hump and the 6.4 keV fluorescence line are clearly detectable in both sets of observations. Since both the equivalent width of the iron line and the relative reflected fraction of continuum are higher during lower flux states, we conclude that two reflection components are present in NGC 5506.

In Section 2 we describe the observations and the analysis of the *RXTE* data. The results of our spectral modelling are presented in Section 3. In Section 4 we then describe the variability of the spectral parameters and show that the observed spectral vari-

<sup>★</sup> E-mail: gl@astro.soton.ac.uk

ability can be described by a model involving both disk and torus reflection.

## 2 OBSERVATIONS AND DATA ANALYSIS

*RXTE* observed NGC 5506 with the Proportional Counter Array (PCA) and the High Energy X-ray Timing Experiment (HEXTE) instruments. The PCA (Zhang et al. 1993) consists of 5 Xenon-filled Proportional Counter Units (PCUs), sensitive to X-ray energies from 2-60 keV. The maximum effective area of the PCA is  $6500 \text{ cm}^2$ . The HEXTE (Rothschild et al. 1998) covers the energy range 15-250 keV with a maximum effective area of  $1400 \text{ cm}^2$ . We have observed NGC 5506 with the *RXTE* since May 1996 as part of a long term monitoring campaign of 4 Seyfert galaxies. We used short ( $\sim 1$  ksec) observations separated by a range of time intervals. During 1996 the source was observed twice daily for 10 days, daily for 32 days, and weekly for 13 weeks. Since November 1996 the monitoring has continued with observations every two weeks. The monitoring data presented here cover  $\sim 1000$  days within the gain epoch 3 of the PCA instrument and amount to 77 ksec of good exposure time. We also observed NGC 5506 between 20 June 1997 and 9 July 1997 with *RXTE* for 91 ksec. See Fig. 1 for the distribution of observations during both campaigns.

We have used FTOOLS V4.2 for the reduction of the PCA and HEXTE data. PCA “good times” have been selected from the Standard 2 mode data sets using the following criteria: target elevation  $> 10^\circ$ , pointing offset  $< 0.01^\circ$ , time since SAA passage  $> 30$  min, standard threshold for electron contamination. Since the PCUs 4 and 5 are often switched off, only the data from the PCUs 0, 1, and 2 have been included. Spectra and light curves were extracted from the top Xenon layer data.

We calculated the background in the PCA with the tool PCABACKEST V2.1 using the L7 model for faint sources, which is suitable for determining the PCA background for energies  $\leq 24$  keV. In the case of NGC 5506, the PCA background dominates over the source spectrum at energies  $> 15$  keV. Therefore correct background subtraction is crucial for the determination of the reflected fraction of the source spectrum from the strength of the reflection hump at energies  $> 10$  keV. In order to test the accuracy of the background model we analysed 100 PCA blank field pointings from observation P30801. We performed the data reduction and background estimation for the blank field pointings in the same manner as for the NGC 5506 science data and produced a set of background subtracted spectra including PCUs 0-3. From this set of spectra we derived the intrinsic standard deviation in each spectral channel by deconvolving the measured variance with the Poisson errors in the respective channel. The result represents the  $1\sigma$  systematic error in the spectra due to inaccurate background subtraction. Figure 2 shows a comparison of a spectrum selected from the faintest states of NGC 5506 ( $\text{cr} < 21$  cts/sec, see Section 4) and the  $1\sigma$  background standard deviations. The systematic errors are generally smaller than the Poisson errors in the respective channels. We added a typical background subtracted blank field spectrum to the above mentioned faint state spectrum and fitted the PEXRAV models described below to the original and the modified spectrum. The resulting change in the spectral parameters is  $\Delta\Gamma = -0.018$  for the spectral index or  $\Delta R = 0.14$  for the reflected fraction. Note that the flux selected spectra discussed in Section 4 are averaged from many pointings and therefore inaccurate background subtraction in individual pointings should have only negligible influence on the results derived from these spectra.

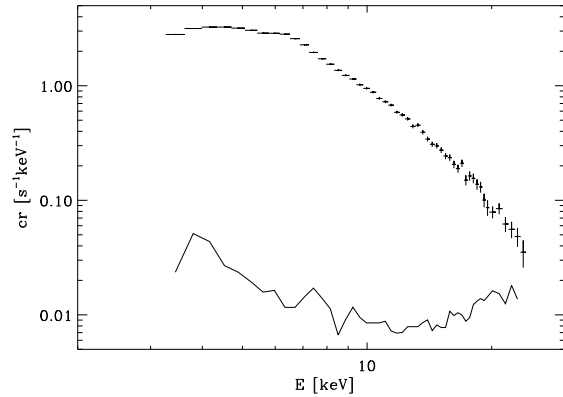


**Figure 2.** Comparison of a spectrum (data points) from the lowest states of NGC 5506 during the long term monitoring ( $\text{cr} < 21$  cts/sec, see Section 4) and the standard deviations in a set of background subtracted spectra of a blank field (solid line). The curve of standard deviations has been smoothed for graphical representation.

Spectral fitting was performed using XSPEC V10.0 using the latest releases of the detector response matrices. All observations reported here have been carried out during the PCA gain epoch 3. However, small temporal gain variations lead to changes in the detector response within this epoch. In order to account for these changes we used the tool PCARSP V2.37 to create individual response matrices for the June 1997 observation and for each of the monitoring observations.

The inter-calibration of PCA and HEXTE regarding the normalization of the spectrum is still uncertain and the relatively low count rate (2 cts/s per cluster) for NGC 5506 in the HEXTE detectors prevents an accurate measurement of the spectral slope in the HEXTE band alone. Therefore the inclusion of the HEXTE spectra in the fitting did not significantly improve the constraints on spectral parameters and we only present the results of the PCA observations here. Since the spectral calibration of the softest PCA channels is somewhat uncertain and the L7 background model is not recommended for energies above 24 keV, we only use the PCA data between 3 keV and 24 keV.

For the modelling of the spectrum we use the XSPEC PEXRAV code (Magdziarz & Zdziarski 1995) which calculates a power law with exponential cutoff at high energies reflected by a slab of neutral material. The iron emission feature is modeled by a Gaussian line. The spectrum in the PCA energy range is only marginally affected by photoelectric absorption and by the high energy cutoff of the underlying power law. Perola (1998) measured the X-ray spectrum of NGC 5506 in the broader energy range of the *BeppoSAX* instruments and find that the absorbing column density of the host galaxy is  $N_{\text{H}} = 3.6 \cdot 10^{22} \text{ cm}^{-2}$ . Their lower limit for the high energy cutoff is  $E_{\text{max}} = 300 \text{ keV}$ . In the following we adopt their values for  $N_{\text{H}}$  and  $E_{\text{max}}$ .

The reflected fraction  $R$  is defined as  $R = \Omega/(2\pi)$  where  $\Omega$  is the solid angle subtended by the reflector as seen from the X-ray source. In the case of an infinite flat disk as reflector  $R = 1$  would be expected. The intensity of the reflected component also strongly depends on the inclination of the reflecting slab. However, it is not possible to simultaneously constrain both inclination and the reflective fraction  $R$ . We therefore adopted an inclination of  $40^\circ$  as suggested by the profile of the iron  $\text{K}\alpha$  fluorescence line

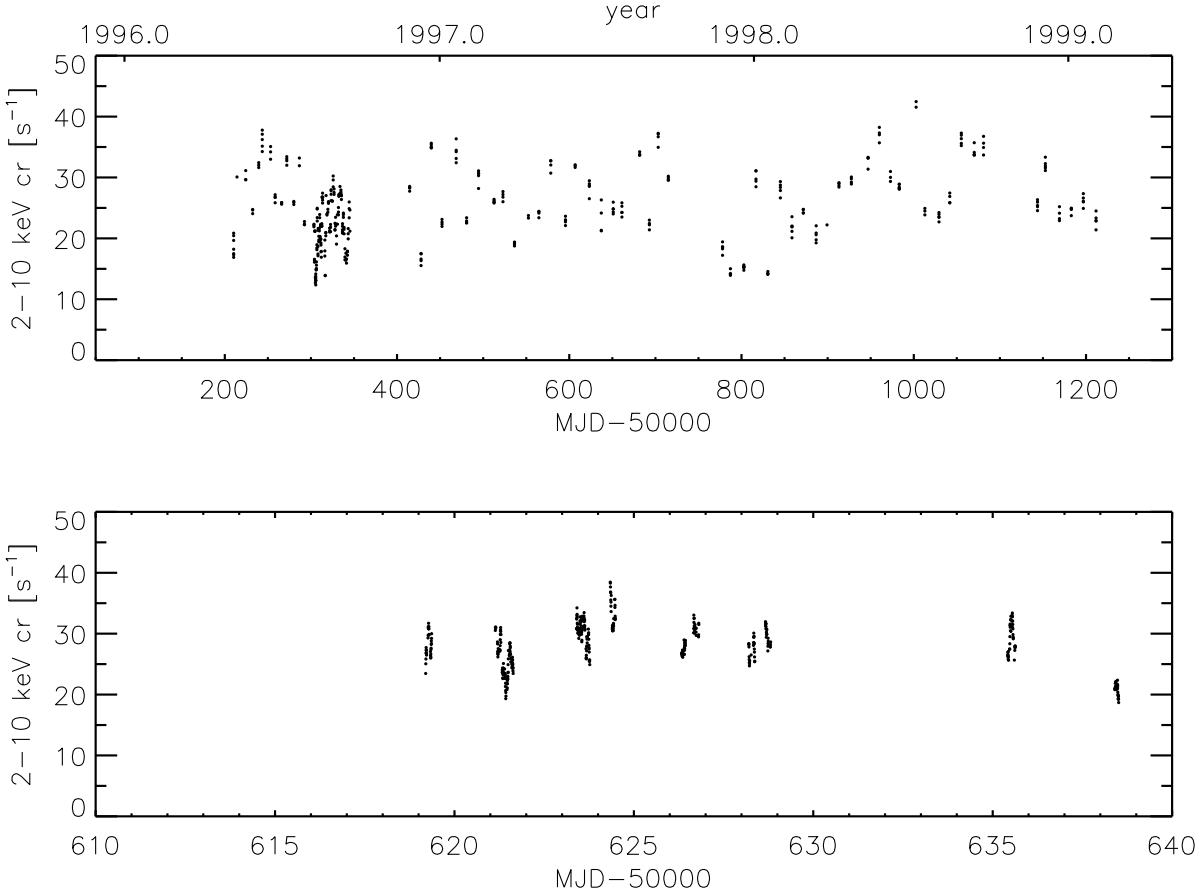


**Figure 1.** RXTE Background subtracted PCA 2-10 keV lightcurves during the long term monitoring campaign (upper panel) and the June 1997 observations (lower panel). Data from PCUs 0-2 have been added, the binning is 256 sec. The errors in the count rates are generally  $< 0.5\text{s}^{-1}$ , comparable to the size of the plot symbols. Note that apparently simultaneous data points in upper plot correspond to several time bins within one observation, these data points give an indication on the short time variability of the source.

measured by ASCA (Wang et al. 1999). All elementary abundances were set to the solar values.

In order to investigate whether the flux variability of NGC 5506 is accompanied by spectral changes, we have accumulated PCA spectra during epochs of similar source count rates in the 2-10 keV lightcurves as shown in Fig. 1. For the June 1997 observations we set the ranges  $< 24$  cts/sec,  $24\text{-}27$  cts/sec,  $27\text{-}30$  cts/sec,  $> 30$  cts/sec. For the monitoring observations, where the spread in count rates is larger, 6 ranges have been chosen:  $< 21$  cts/sec,  $21\text{-}24$  cts/sec,  $24\text{-}27$  cts/sec,  $27\text{-}30$  cts/sec,  $30\text{-}33$  cts/sec, and  $> 33$  cts/sec.

Since the detector response matrices of the PCA change over the time span of the monitoring observations, we have produced response matrices for each flux selected spectrum. These matrices have been constructed by averaging the matrices of the individual observations using weight factors according to the exposures contributing to the final spectra.

Each of the spectra was the fitted with a PEXRAV + GAUSS model as discussed above, the results on spectral variability are given in Section 4.

### 3 X-RAY SPECTRA

A fit of the time averaged PCA spectrum from the June 1997 observation with a simple power law model shows the presence of a strong Fe K $\alpha$  emission line and a significant reflection component at energies above  $\sim 10$  keV (see Fig. 3).

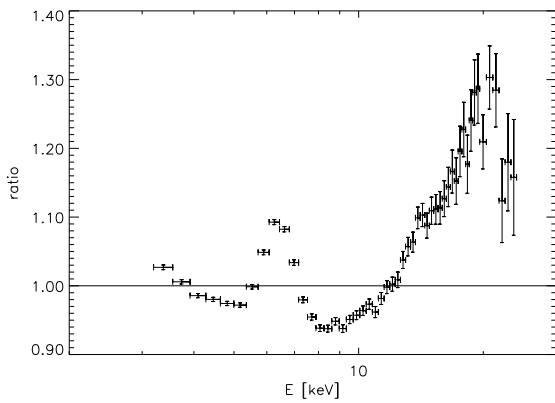
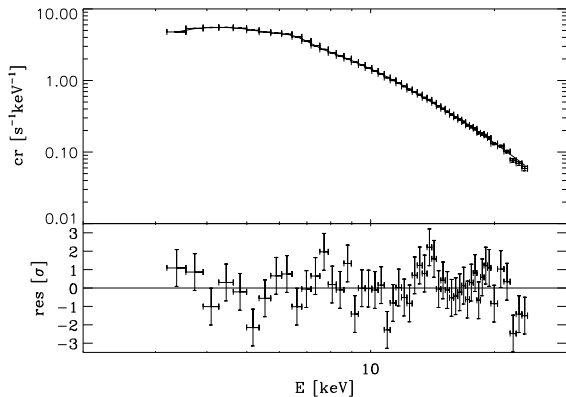
The combination of the PEXRAV model and a Gaussian iron line results in a satisfactory fit to the high signal to noise spectrum. The iron line is slightly resolved with  $\sigma \sim 0.30^{+0.03}_{-0.06}$  keV, but there is no evidence for any gravitational redshift. The best fit energy is  $6.404^{+0.024}_{-0.023}$  keV in the source frame of NGC 5506. This is consistent with higher resolution ASCA spectroscopy by Wang et al. (1999), who report  $\sigma=0.2$  for a single Gaussian profile and no gravitational redshift of the iron K $\alpha$  line.

The best fit value for the reflected fraction during the June 1997 observation is  $R = 1.2 \pm 0.08$ . This is in good agreement with the value measured by *BeppoSAX* in January 1997 ( $R = 1.05 \pm 0.58$ , Perola 1998) and is near the value  $R = 1$  that would be expected for the case of a simple geometry with a large disk reflecting the primary X-rays.

For the best fit PEXRAV model the absorbed 2-10 keV flux is  $1.02 \cdot 10^{-10}$  erg cm $^{-2}$ s $^{-1}$ , the corresponding X-ray luminosity is  $1.25 \cdot 10^{42}$  erg s $^{-1}$  ( $H_0 = 50\text{Mpc km}^{-1}\text{s}$ ,  $q_0 = 0.5$ ).

**Table 1.** Fit parameters for time-averaged June 1997 spectrum

model	$\Gamma$	line EW [eV]	line $E_{\text{source}}$ [keV]	line $\sigma$ [keV]	$R_{\text{refl}}$	$\chi^2$ (dof)
PWL	$2.00 \pm 0.005$	-	-	-	-	3089 (48)
PWL+GAUSS	$1.85 \pm 0.007$	$248 \pm 15$	$6.265 \pm 0.013$	$0.41 \pm 0.22$	-	726 (45)
PEXRAV	$2.19 \pm 0.008$	-	-	-	$1.766 \pm 0.064$	1781 (48)
PEXRAV+GAUSS	$2.13^{+0.01}_{-0.01}$	$149^{+9}_{-6}$	$6.404^{+0.024}_{-0.023}$	$0.302^{+0.032}_{-0.058}$	$1.20^{+0.08}_{-0.08}$	52.7 (45)

**Figure 3.** Ratio of data to model when a simple power law spectrum is fitted to the June 1997 PCA spectrum of NGC 5506. Both the iron K $\alpha$  line and a reflection hump are obvious in the residuals.**Figure 4.** RXTE PCA spectrum fitted with a PEXRAV+GAUSS model. See Table 1 for the model parameters.

#### 4 SPECTRAL VARIABILITY

In our monitoring data from NGC 5506 we see variations in the 2–10 keV count rate between 12 cts/sec and 42 cts/sec. During the June 1997 observations the source varied between 19 cts/sec and 39 cts/sec. We analysed the hardness-ratios between different bands of the PCA energy range and found that the flux variations are accompanied by variations in the spectral hardness: the spectrum appears to be softer during epochs of higher flux. This spectral behaviour has been observed in a number of other Seyfert galaxies before (e.g. M'Hardy et al. (1998), Uttley et al. (1998), Chiang et al. (2000)). In the framework of the reflection models there are two possibilities to explain an anti-correlation of source flux and spectral hardness:

1. The intrinsic spectrum of the primary X-ray source might soften during high flux states.

2. As the primary X-ray source weakens, the fraction of reflected radiation might increase, e.g. due to a time lag between the primary and reflected components.

In order to investigate these possibilities we fitted count rate selected spectra (as described in Section 2) with the PEXRAV (Magdziarz & Zdziarski 1995) model and a Gaussian emission line. No significant variability of the source frame energy or the width  $\sigma$  of the iron fluorescent line have been found. Therefore these parameters have been fixed to values compatible with any of the single fits,  $E_{\text{source}} = 6.4$  keV and  $\sigma = 0.35$  keV. The results of the spectral fits are shown in Table 2. The variations of intrinsic photon index, reflected fraction, and iron line flux with the count rate are shown in Figure 5. During the June 1997 observations the spectral index was  $\Gamma \sim 2.13$  and did not vary with flux. On the longer time scales of the monitoring observations, however, an anti-correlation of flux and hardness of the intrinsic power law is clearly visible. It is not clear whether the difference between the two data sets regarding the variation of the spectral index is due to the different time scales of the observations. An analysis of the interval of more intense monitoring between MJD=50300 and MJD=50350 showed that during this interval the source showed the same spectral index variability as during the long term monitoring campaign as a whole.

#### 4.1 Reflection and iron fluorescence emission

The results on the reflected fraction for both the long term and the intense monitoring are consistent with each other and show tentative evidence for an anti-correlation of the reflected fraction  $R$  with source flux. Figure 6 shows 68% and 90% contours for the parameters  $\Gamma$  and  $R$ . On the shorter time scales of the June 1997 observations the changes in reflected fraction  $R$  contribute to the variability in spectral hardness, while on longer time scales variations of the intrinsic power law index  $\Gamma$  seem to be the main cause of the spectral variability. Variability of the intrinsic spectral index was found to be the source of spectral variability in the cases of NGC 5548 (Chiang et al. 2000) and MCG–6–30–15 (Lee et al. 1999). Although the best fit values of the reflected fraction for the different flux states in the long term monitoring are formally consistent with each other, an anti-correlation with the source flux is present. Zdziarski et al. (1999) report a *positive* correlation of  $\Gamma$  and  $R$  in samples of Seyfert galaxies and X-ray binaries and claim that this correlation also holds for the spectral variability of individual sources. Our results on NGC 5506 are in contrast to these findings, as  $\Gamma$  and  $R$  are anti-correlated during the long term monitoring observations. Zdziarski et al. (1999) explain the  $R(\Gamma)$  correlation as follows: The power law X-ray spectra arises in a hot Comptonizing plasma surrounding a cool accretion disk. Cooling of plasma by soft photons from the disk affects the spectral index.

The correlation of  $R$  and  $\Gamma$  is likely, as both the strength of the reflection and the flux of cooling photons depend on the properties of the disk. The absence of this correlation in the spectral variability of NGC 5506 means that either the corresponding properties of the accretion disk are not variable in this source or the effect on the reflected fraction is compensated for by reflection from the torus discussed in Section 4.2.

Note that the anti-correlated variations in  $R$  and  $\Gamma$  presented here cannot be artifacts of the spectral fitting procedure, which may cause fake correlations between two parameters in the direction of the major axes of the corresponding error ellipses. Spurious variations in  $R$  and  $\Gamma$  due to their degeneracy in the PEXRAV model would result in a positive correlation. In fact the anti-correlation of  $R$  and  $\Gamma$  requires real variations in the hardness of the X-ray spectrum.

During the long term monitoring the iron line flux does increase with the continuum flux, but slower than proportionally as is obvious from the decreasing values of the equivalent width. The spectra from June 1997 do not show significant variations of the iron line flux, but the values are consistent with the results from the long term monitoring. Therefore it is not clear whether the iron line flux is actually constant on shorter time scales or whether the variations are not detectable due to the narrower range of flux states during June 1997. The bottom panel of Figure 5 shows a significant increase of the iron line equivalent width at low source flux levels. This is indicative of a constant component the iron  $K\alpha$  line.

#### 4.2 Disk and torus reflection

The variations of reflected fraction and iron line flux with the continuum flux indicate that two reflectors contribute to the reflection hump and the iron line. One reflector, most likely the accretion disk, is close to the central source and responds rapidly to changes in the primary X-ray source. A second reflection component, the tentative torus component, arises from matter more distant from the central source and hence is constant on the observed time scales.

Using the PEXRAV+GAUSS model we have simulated X-ray spectra for a scenario assuming the following components:

1. Variable reflection that is proportional to the current intrinsic flux with the reflected fraction  $R_{\text{disk}}$ .
2. Constant reflection of an intrinsic source whose luminosity corresponds to the average luminosity of the central X-ray source. The reflected fraction is  $R_{\text{torus}}$ .
3. Each of the reflection components are accompanied by iron  $K\alpha$  fluorescence emission. The ratios of reflected continuum flux and fluorescence flux are assumed to be the same in both components.

From a set of simulated spectra with various power law normalizations the total count rates and line equivalents widths have been determined and the variations of the model parameters have been compared with the observed values. The free parameters  $R_{\text{disk}}$ ,  $R_{\text{torus}}$ , and fluorescence yield have been adjusted so that the simulations match the observations. The solid lines in Figure 5 show the simulations with  $R_{\text{disk}} = 0.7$  and  $R_{\text{torus}} = 0.5$ . The fluorescence yield corresponds to an equivalent width of 103 eV for the disk reflection component alone. If the disk covers  $\Omega = 2\pi$  of the sky as seen from the source,  $R_{\text{disk}} = 1$  would be expected. For disk reflection with inclination  $i = 40^\circ$  and an intrinsic power law index of  $\Gamma = 2.1$  George & Fabian (1991) calculated  $EW_{K\alpha} = 120$  eV. Hence, both  $R$  and  $EW_{K\alpha}$  from the disk component are of the right magnitude and the iron abundance is consistent with the solar value.

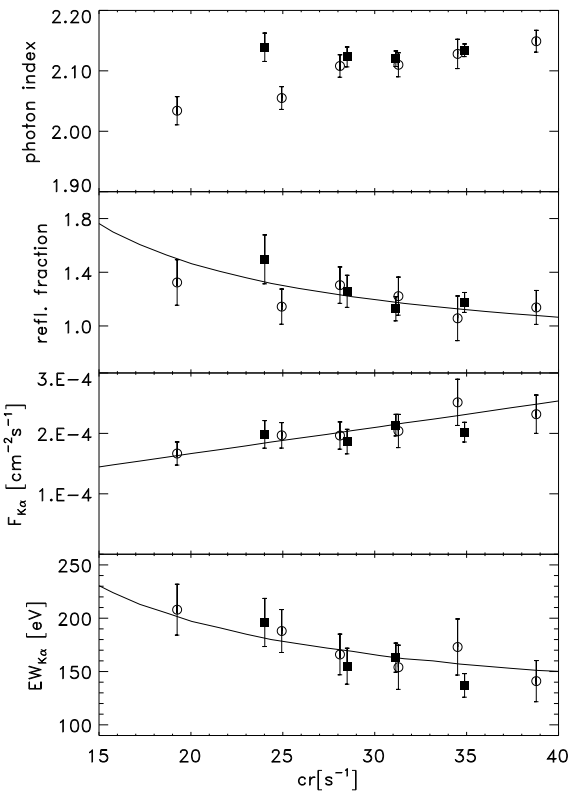


**Figure 5.** Best fit PEXRAV model parameters as functions of the count rate. From top to bottom: photon index  $\Gamma$ , reflected fraction  $R$ , iron line flux, and iron line EW. Filled squares: Results from June 1997 observations. Open circles: Monitoring observations. The lines indicate the values of reflected fraction and line fluxes expected from a model with two reflectors: One close to the primary X-ray source and a more distant reflector leading to a non-variable reflected component (see Section 4.2).

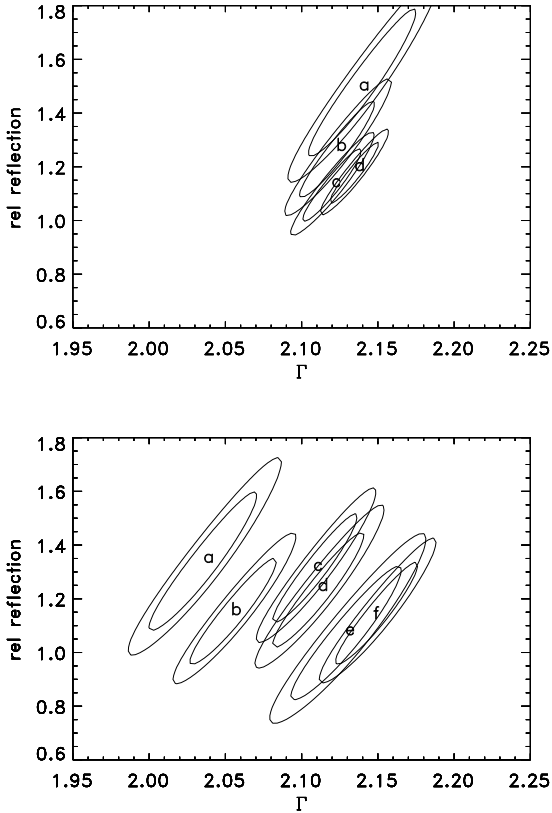
According to our simulations the torus contributes an iron  $K\alpha$  component of  $EW = 75$  eV when the source luminosity is at intermediate levels. This is in good agreement with the strengths of the narrow Fe  $K\alpha$  components found in ASCA spectra of NGC 5506 (66 - 84 eV, Wang et al. 1999) and in a sample of other Seyfert 1.9 - 2 galaxies ( $< EW > = 60$  eV, Weaver et al. 1997). This and the satisfactory fit to the observed spectral variability makes the disk+torus reflection scenario a likely model for NGC 5506. A single reflection component either from the disk or from the torus is not consistent with the observed spectral variability. Figure 7 shows the reflected fraction  $R$  and iron line flux as functions of the count rate for 3 different models: the combined disk+torus reflection model as discussed above (solid lines), a single torus reflector (dotted lines), and prompt reflection from the accretion disk only (dashed lines). The combined  $\chi^2$  values when compared to the measured values of  $R$  and  $F_{K\alpha}$  are  $\chi^2/dof = 12.2/17$  for the ‘disk+torus’ model,  $\chi^2/dof = 56.6/18$  for the ‘torus only’ model, and  $\chi^2/dof = 29.3/18$  for the ‘disk only’ model.

## 5 CONCLUSION

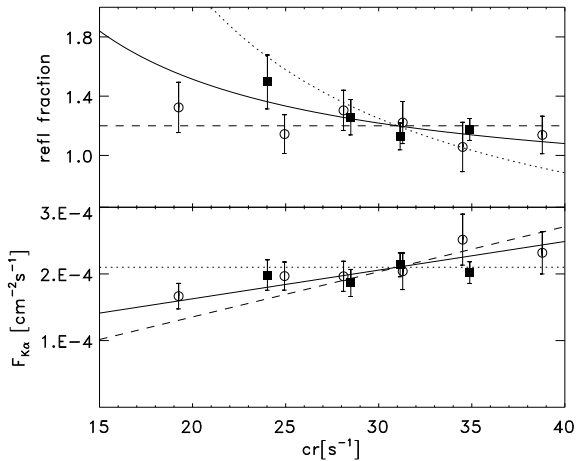
We show that the variability of the reflected continuum and the Fe  $K\alpha$  fluorescence emission in the Seyfert 2 galaxy NGC 5506 are

**Table 2.** Count rate selected spectra

count rate [ $s^{-1}$ ]	exposure [s]	$\Gamma$	line EW [eV]	$R_{\text{refl}}$	$\chi^2$ (dof)
June 1997					
< 24	14592	$2.139 \pm 0.023$	$196 \pm 23$	$1.496 \pm 0.182$	34.5 (47)
24-27	19760	$2.123 \pm 0.016$	$155 \pm 17$	$1.258 \pm 0.120$	32.6 (47)
27-30	26352	$2.120 \pm 0.013$	$163 \pm 14$	$1.128 \pm 0.090$	34.0 (47)
> 30	33744	$2.134 \pm 0.010$	$137 \pm 11$	$1.175 \pm 0.074$	42.0 (47)
Long term monitoring					
< 21	18112	$2.040 \pm 0.024$	$207 \pm 24$	$1.358 \pm 0.173$	42.8 (47)
21-24	16688	$2.059 \pm 0.019$	$194 \pm 20$	$1.172 \pm 0.133$	39.3 (47)
24-27	15616	$2.113 \pm 0.019$	$172 \pm 19$	$1.334 \pm 0.138$	35.7 (47)
27-30	11168	$2.114 \pm 0.020$	$154 \pm 21$	$1.247 \pm 0.144$	29.9 (47)
30-33	6064	$2.132 \pm 0.024$	$165 \pm 26$	$1.080 \pm 0.168$	23.0 (47)
> 33	9488	$2.152 \pm 0.018$	$145 \pm 19$	$1.158 \pm 0.128$	43.6 (47)

**Figure 6.** 68% and 90% confidence contours for the parameters  $R$  (relative reflection) and  $\Gamma$  (photon index) of the PEXRAV model. *Top:* Count rate selected spectra from June 1997 observation, a)  $< 24 s^{-1}$ , b)  $24..27 s^{-1}$ , c)  $27..30 s^{-1}$ , d)  $> 30 s^{-1}$ . *Bottom:* Count rate selected spectra from monitoring observations, a)  $< 21 s^{-1}$ , b)  $21..24 s^{-1}$ , c)  $24..37 s^{-1}$ , d)  $27..24 s^{-1}$ , e)  $30..33 s^{-1}$ , f)  $> 33 s^{-1}$ .

well described by a model that assumes reprocessing by both an accretion disk and a distant medium, which might be the molecular torus. In contrast to the monitoring observations of NGC 4051 (Uttley et al. 1999), no long lasting states of low X-ray flux have been observed for NGC 5506. Therefore the distance of the reflect-

**Figure 7.** Best fit parameters  $R$  and  $F_{K\alpha}$  as in Fig. 5. The solid lines indicate the “two reflectors” model described in Section 4.2. The dotted lines show the expected slopes for a single distant reflector, the dashed lines represent a model with prompt reflection

ing matter from the central X-ray source is not well constrained in this case. However, the time delay of  $> 150$  days found for a similar constant reflection component in NGC 4051 (Uttley et al. 1999) supports the torus hypothesis.

The relative contributions of the disk and the torus are approximately equal during the lowest flux states we have observed. When the X-ray luminosity is intermediate to high, reprocessing in the accretion disk dominates the reflected continuum and the iron line. The strength of the reflection features from the accretion disk alone is broadly consistent with an inclination angle  $i = 40^\circ$  as inferred from ASCA measurements (Wang et al. 1999) of the Fe  $K\alpha$  profile. At this inclination the observed X-ray absorption ( $N_H = 3.6 \cdot 10^{22} \text{ cm}^{-2}$ , Perola 1998), which is within the range for Seyfert 2 galaxies, but towards the lower end (Turner & Pounds 1989) might be well below the total column density of the torus. The torus contribution to the Fe  $K\alpha$  fluorescence as inferred from our variability study is in very good agreement with ASCA spectroscopy of the line profile (Wang et al. 1999).

We conclude that long term monitoring of AGN is an excellent

method to study the geometry of their inner regions as it has the potential to actually measure the linear scales of the components contributing to reprocessing.

## REFERENCES

Chiang J., Reynolds C.S., Nowak M.A., et al. 2000, *ApJ*, 528, 292  
 de Vaucouleurs G., de Vaucouleurs A., and Corwin H., 1976, *Second Reference catalogue of Bright Galaxies*, University of Texas Press, Austin  
 George I.M., and Fabian A.C., 1991, *MNRAS*, 249, 352  
 Ghisellini G., Haardt F., and Matt G., 1994, *MNRAS*, 267, 743  
 Goodrich R.W., Veilleux S., and Hill, G.J., 1994, *ApJ*, 422, 521  
 Guainazzi M., Nicastri F., Fiore F., et al., 1998, *MNRAS* 301, L1  
 Krolik J.H., Madau P., Źycky P.T., *ApJ*, L57  
 Lee J.C., Fabian A.C., Reynolds C.S., Brandt W.N., and Iwasawa K., 1999, *MNRAS* submitted  
 Magdziarz P., and Zdziarski A., 1995, *MNRAS*, 273, 837  
 M<sup>c</sup>Hardy I.M., Uttley P., M<sup>c</sup>Hardy I.M., Papadakis I.E., 1998, *Nuclear Physics B* (Proc. Suppl.), 69/1-3, 510  
 Nandra K., George, I.M., Mushotzki, R.F., Turner, T.J., Yaqoob, T., 1997, *ApJ*, 488, L91  
 Perola G.C., 1998, *Nuclear Physics B* (Proc. Suppl.), 69/1-3, 477  
 Pounds, K.A., Nandra, K., Steward, G.C., George, I.M., and Fabian, A.C., 1990, *Nature*, 344, 132  
 Reynolds, C.S., and Begelman, M.C., 1997, *ApJ*, 488, 109  
 Rothschild R.E., Blanco P.R., Gruber D.E., et al. 1998, *ApJ*, 496, 538  
 Tanaka, Y., Nandra, K., Fabian, A.C. et al., 1995, *Nature*, 375, 659  
 Turner T.J., and Pounds K.A., 1989, *MNRAS*, 240, 833  
 Uttley P., M<sup>c</sup>Hardy I.M., Papadakis I.E., Cagnoni, I., Fruscione A., 1998, *Nuclear Physics B* (Proc. Suppl.), 69/1-3, 490  
 Uttley P., M<sup>c</sup>Hardy I.M., Papadakis I.E., Guainazzi M., Fruscione A., 1999, *MNRAS*, 307, L6  
 Veilleux S., Goodrich R.W., and Hill G.J., 1997, *ApJ*, 477, 631  
 Wang T., Miura T., Otani C., Matsuoka M., and Awaki H., 1999, *ApJ*, 515, 567  
 Weaver K.A., Yaqoob T., Mushotzky R.F., Nousek J., Hayashi I., and Koyama K., 1997, *ApJ*, 474  
 Weaver K.A., and Reynolds C.S., 1998, *ApJ*, 503, L39  
 Wilson A.S., Penston M.V., Fosbury R.A.E., and Boksenberg A., 1976, *MNRAS*, 177, 673  
 Wilson A.S., Baldwin J.A., and Ulvestad J.S., 1985, *ApJ*, 291, 627  
 Yaqoob T., Serlemitsos P.J., Turner T.J., George I.M., and Nandra K., 1996, *ApJ*, 470, L27  
 Zdziarski A.A., Lubinski P., and Smith D.A., 1999, *MNRAS*, in press  
 Zhang W., Giles A.B., Jahoda K., Soong Y., Swank J.H., and Morgan E.H., 1993, In Siegmund O.H., ed., EUV, X-ray, and Gamma-ray Instrumentation for Astronomy IV, SPIE, Bellingham WA, p. 324